

First-Principles Quantum Chemical Studies of Porphyrins

ABHIK GHOSH*

Department of Chemistry, Faculty of Science,
University of Tromsø, N-9037 Tromsø, Norway, and
San Diego Supercomputer Center, 10100 Hopkins Drive,
La Jolla, California 92093

Received August 25, 1997

Introduction

Porphyrins are perhaps best known for their biological functions and coordination chemistry.¹ With their high molecular symmetry (up to D_{4h}) and rich electronic absorption properties, porphyrins (Figure 1) have been extensively studied by quantum chemists. During the 1970s, semiempirical calculations resulted in important insights into the electronic structure and spectra of porphyrins.² While such calculations continue to be useful, especially for studies of porphyrin excited states, recent advances in quantum chemical and computer technologies permit more accurate *ab initio* or first-principles calculations on large porphyrin-sized molecules. However, most porphyrin chemists do not consider *ab initio* calculations as a practical tool in their research. A goal of this Account is to encourage a change in this state of affairs. Two areas are chosen for discussion. In the first part of this Account, we will focus on recent advances in calculations of porphyrin ionization potentials (IPs). Information from electrochemistry and photoelectron spectroscopy are integrated with theoretical results to develop a unified picture of substituent effects (SEs) in porphyrins. In the second part of this Account, we will evaluate the role that first-principles methods can play in structural studies of porphyrin-type molecules.

Ionization Potentials of Porphyrins and Related Molecules

Since the late 1980s, many novel substituted porphyrins such as β -perhalogenated porphyrins and porphyrins with multiple perfluoroalkyl and nitro groups have been synthesized.³ Compared to ordinary metalloporphyrins, metal complexes of some of the new electron-deficient porphyrins have proved to be stable and efficient catalysts of

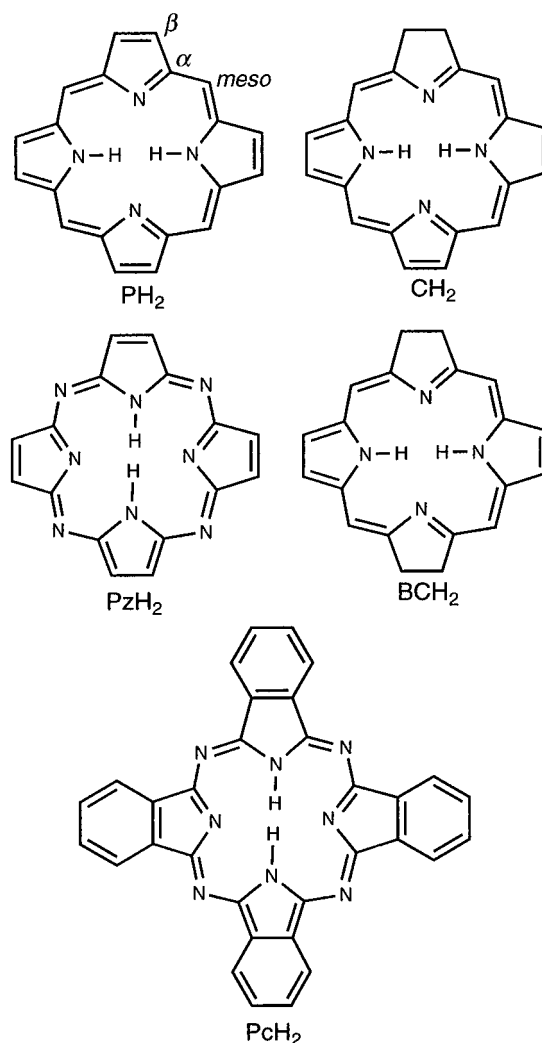


FIGURE 1. Some basic porphyrinic structures: PH₂, porphyrin; CH₂, chlorin; BCH₂, bacteriochlorin; PzH₂, porphyrazine; PcH₂, phthalocyanine.

various oxygenation reactions.^{3,4} These findings prompted us to seek a detailed analysis of SEs in porphyrins. We chose a combined theoretical and experimental approach involving *ab initio* calculations and X-ray photoelectron spectroscopy (XPS), while other groups focused on electrochemical measurements. A recent synthesis of the data available from these diverse sources has resulted in a broad self-consistent picture of substituent effects on ionization and oxidation potentials of porphyrins.⁵

Early Results From Hartree–Fock Calculations. *Ab initio* Hartree–Fock (HF) theory,^{6,7} appeared to be a reasonable choice for an initial first-principles exploration of porphyrin IPs. According to Koopman's theorem (KT), IPs are given by the sign-reversed orbital energies for the occupied orbitals of a closed-shell molecule. The assumption here is that the molecular orbitals do not relax as a result of ionization. Also, electron correlation is not

Abhik Ghosh, born 1964, did his undergraduate studies at Jadavpur University, India, and his doctoral research with Paul Gassman and Jan Almlöf at the University of Minnesota. After postdoctoral research with Lawrence Que in Minnesota and with David Bocian in California, he became and continues to be an Associate Professor of chemistry at the University of Tromsø, Norway. He is also a Senior Fellow of the San Diego Supercomputer Center. His research focuses on porphyrins, bioinorganic chemistry, and computational chemistry.

* Address correspondence to the University of Tromsø.

Table 1. Five Lowest One-Electron IPs (eV) of PH₂ and β -Octaalkylporphyrins for Different Methods and Basis Sets

symmetry	PH ₂						octaalkylporphyrin		
	HF-KT ^a			LDF ^b	NLDFT ^b	exptl ^c	HF-KT ^d		exptl ^c
	DZ	DZP	TZDP	TZP	TZP		DZ	DZP	
² B _{1u}	6.44	6.78	6.77	7.18	6.99	6.9	6.19	6.64	6.39
² A _u	6.23	6.22	6.15	7.36	7.17	7.2	5.80	6.72	6.83
² B _{2g}	8.89	9.07	9.04	8.14	7.93	8.1	8.18		7.80
² B _{1u}	9.13	9.28	9.24		"7.96" ^f	8.3	8.32		8.13
² B _{3g}	10.16	10.20	10.16	8.82	8.64	8.7	9.50		8.44

^a Reference 6. ^b Reference 16. ^c Experimental results from ultraviolet photoelectron spectroscopy: ref 8. ^d Reference 7. ^e Reference 5. ^f This number is estimated from NLDFT calculations on zinc porphine.¹⁶

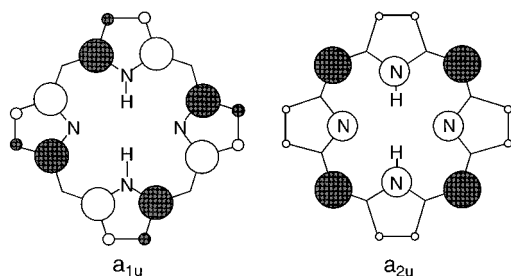


FIGURE 2. Schematic diagram of the two HOMOs of a typical porphyrin.

taken into account in HF theory. The errors due to the neglect of relaxation and correlation effects are of opposite signs and, for low-energy valence ionizations, of comparable magnitude (~ 0.5 eV). Table 1 presents the low-energy HF-KT valence IPs of unsubstituted porphyrin (PH₂)⁶ and β -octamethylporphyrin⁷ and compares them to ultraviolet photoelectron spectroscopic (UPS)⁸ data. Overall, the HF-KT IPs do not change much on improvement of the basis set beyond double- ζ (DZ) or double- ζ plus polarization (DZP) quality.^{6,7} The HF orbital energy spectra reproduce the qualitative clustering patterns of the UPS peaks. For both PH₂ and octaalkylporphyrin, HF theory reproduces the experimental finding that the two lowest IPs are energetically well-separated from all other IPs. This is expected from Gouterman's four-orbital model of porphyrin electronic spectra, according to which (i) the two HOMOs of a typical porphyrin are near-degenerate (Figure 2) as are the two LUMOs and (ii) these four orbitals are energetically well-separated from other occupied and virtual orbitals.⁹ The calculations also reproduce in a semiquantitative manner the experimentally observed electronic effect of β -octaalkyl substitution (ca. 0.5 eV) on the lowest IP(s) of PH₂.⁷

For higher-energy IPs, relaxation energies can be as large as several electronvolts, and the difference in correlation energies between the neutral and ionized states is much smaller. Thus, the theoretical and experimental XPS core electron binding energy scales are shifted relative to each other by a "systematic error" for a series of related molecules. For example, HF theory accurately reproduces differences in N 1s IPs of the various nitrogens in the porphyrin and porphyrazine ring systems (Figure 3).^{10,11} For PH₂, the experimental core IPs of the protonated nitrogens exceed those of the unprotonated nitrogens by 2.1 eV, compared to an HF/DZP value of 1.89 eV.¹⁰ HF theory also reproduces the electron-withdrawing effect

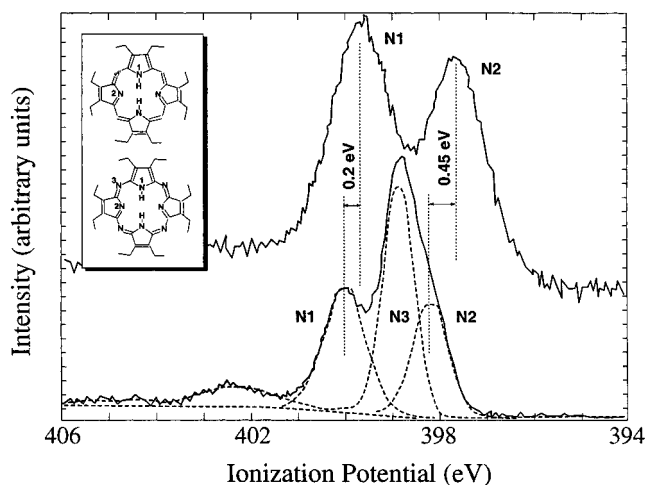


FIGURE 3. Nitrogen 1s XPS of octaethylporphyrin and octaethylporphyrazine.

Table 2. HF and XPS Shifts (eV) in the Nitrogen 1s Core IPs of Several Free-Base Tetraphenylporphyrins, with TPPH₂ as Zero Level^{a,b} (Reprinted with Permission from Reference 7. Copyright 1992 American Chemical Society)

porphyrin	HF	XPS
<i>meso</i> -tetraphenylporphyrin	0.00	0.0
<i>meso</i> -tetrakis(2,6-dichlorophenyl)porphyrin	0.10	0.4
<i>meso</i> -tetrakis(4-cyanophenyl)porphyrin	0.79	0.6
<i>meso</i> -tetrakis[4-(trifluoromethyl)phenyl]porphyrin	1.90	0.7
<i>meso</i> -tetrakis(4-nitrophenyl)porphyrin	1.01	0.7
<i>meso</i> -tetrakis(pentafluorophenyl)porphyrin	1.27	0.9

^a A higher or more positive number indicates a higher nitrogen core IP, i.e., more electron-deficient nitrogens. ^b Only one theoretical or experimental shift is given per porphyrin, since the energy splitting between the core IPs of the protonated and unprotonated nitrogens is virtually constant at 2.1 eV for all these porphyrins, both theoretically and experimentally.

(0.2–0.45 eV) of *meso*-tetraaza substitution on the N 1s IPs of the porphyrin macrocycle (Figure 3).^{10,11} Table 2 compares HF and XPS shifts in the nitrogen core IPs of several free-base tetraphenylporphyrins as a function of different substitution patterns on the phenyl rings.⁷ The agreement between theory and experiment is semiquantitative. Certain phenyl substitution patterns are seen to strongly modulate the N 1s IPs and, therefore, the electronic character of the central metal-binding region of the porphyrin. Thus, perfluorination of the phenyl rings elevates the nitrogen core IPs by almost a full electronvolt. Similarly, *p*-CN, *p*-CF₃, and *p*-NO₂ substituents on the four phenyl groups of *meso*-tetraphenylporphyrin (TPPH₂) raise

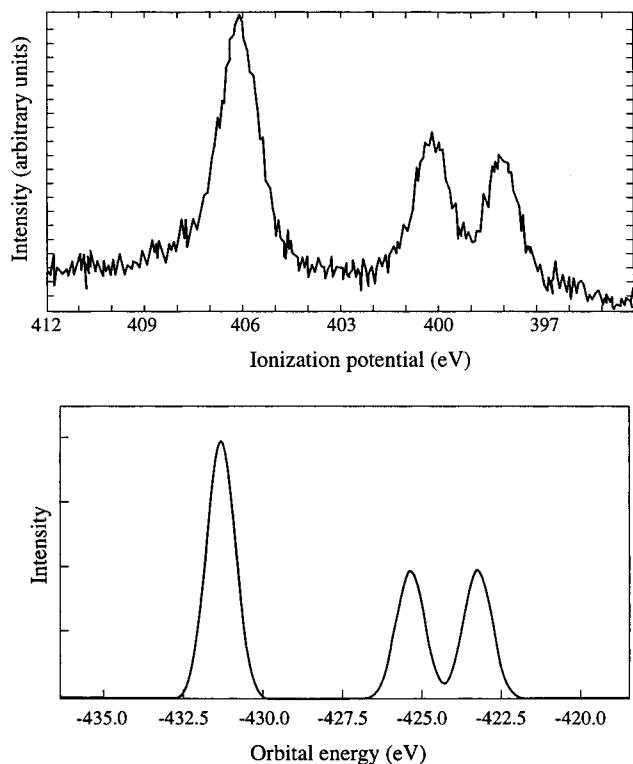


FIGURE 4. Experimental and HF simulated N 1s of T-*p*-NO₂PPH₂.

the core IPs of the central nitrogens by 0.6–0.7 eV.⁷ Figure 4 provides another example of the excellent performance of HF theory: observe how closely the N 1s XPS of *meso*-tetrakis(*p*-nitrophenyl)porphyrin and the corresponding HF simulation agree.⁷

However, there remained certain experimental substituent effect data that simply could not be reconciled with HF predictions. Thus, HF theory grossly overestimates the electronic effects of peripheral halogen substituents on the XPS N 1s IPs and electrochemical oxidation potentials of porphyrins.^{7,12} HF theory also fails to reproduce large electron-donating effects of ca. 0.5 eV of *meso*-tetraphenyl substitution on the valence and N 1s IPs of porphine.^{5,7} HF theory also provides an inaccurate description of the N 1s IPs and hence of the molecular charge distributions of free-base hydroporphyrins such as chlorins and bacteriochlorins.¹³

Performance of Density Functional Theory. To correct these problems, we needed to go beyond the Hartree–Fock approximation and take electron correlation into account. Since the molecules of interest range from about 40 to 100 atoms, the prospect of routine use of *ab initio* correlated methods was unattractive. Fortunately, early explorations with density functional theory (DFT), which can account for electron correlation in an implicit and computationally expedient manner, yielded very promising results. Although DFT is not generally applicable to excited states, it *can* be used for calculations of the lowest-energy state of each symmetry for a particular system.¹⁴ We used local¹⁵ (LDF) and nonlocal¹⁶ DFT to calculate four valence IPs of PH₂, corresponding to the lowest ²A_u, ²B_{1u}, ²B_{2g}, and ²B_{3g} π -ionized states, each IP being equal to the energy difference between the un-

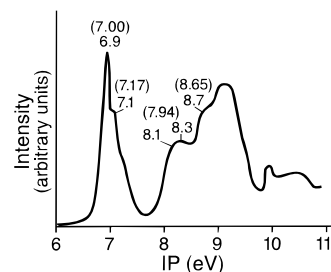


FIGURE 5. UPS of PH₂ reproduced after stylistic modification. Experimental and NLDFT calculated features (eV) are shown outside and within parentheses, respectively.

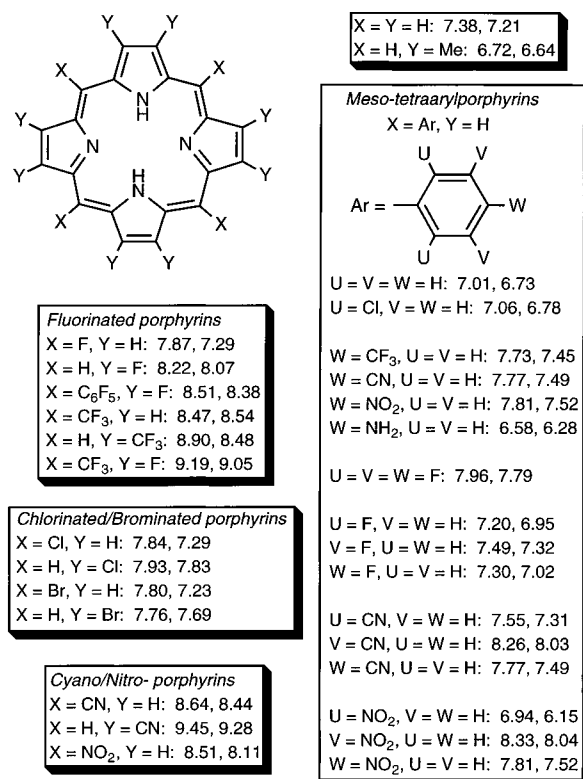


FIGURE 6. The two lowest LDF IPs of diverse substituted porphyrins.

ionized and the appropriate ionized states. Table 1 and Figure 5 compare the DFT IPs with the experimental UPS. Local and nonlocal DFTs reproduce the experimental IPs of PH₂ to within 0.3 and 0.1 eV, respectively.

The two lowest experimental IPs of β -octaethylporphyrin are 6.39 and 6.83 eV, which agree to within 0.1–0.3 eV of the calculated LDF values of 6.64 and 6.72 eV for β -octamethylporphyrin.⁵ The three lowest LDF IPs of TPPH₂ (6.73, 7.01, and 7.67 eV) are in similarly good agreement with experimental values of 6.39, 6.72, and 7.71 eV.⁵ LDF theory also reproduces the electronic effects (~0.5–0.7 eV) of *meso*-tetraphenyl and β -octaalkyl substitution. These DFT results represent near-quantitative agreement between theory and experiment, well beyond what was achieved with large-basis HF calculations. This encouraged us to assemble an extensive database of LDF valence IPs and SEs (Figure 6).⁵

Halogenated Porphyrins. The data in Figure 6 afford important insights into halogen SEs on porphyrins, an important topic in view of extensive applications of

halogenated metalloporphyrins as catalysts for hydrocarbon oxygenation. In contrast to HF results but in agreement with electrochemical measurements, LDF theory predicts that *meso*-tetrahalogenation should result in almost no change in a porphyrin's lowest IP.^{5,12} This appears to result from the cancellation of inductive electron-withdrawing and mesomeric electron-donating effects of the halogen substituents. Evidence for the latter effect is found in the spin density distribution of the ground (${}^2B_{1u}$) state *meso*-tetrachloroporphyrin cation where each chlorine atom carries an unpaired spin population of as much as 0.05.¹² β -Octachlorination or octabromination too results in elevations of 0.4–0.5 eV of a porphyrin's lowest IP at the LDF level, in contrast to dramatically higher electronic effects predicted at the HF–KT level.^{5,12} XPS measurements⁵ show that β -Cl₈ or β -Br₈ substitutions elevate the core IPs of the central nitrogens of a porphyrin by 0.4–0.5 eV, in agreement with the LDF valence SEs. Electrochemical confirmation of these LDF results is somewhat complicated. All known β -Cl₈ or β -Br₈ porphyrins are also *meso*-tetraaryl-substituted and have severely buckled equilibrium geometries. It turns out that macrocycle buckling raises the lowest IPs and thus effectively masks the electron-withdrawing effects of the β -halogens. However, tetraarylporphyrins with only a pair of opposite pyrrole rings halogenated are relatively planar, and the oxidation potentials of these compounds allow an electrochemical determination of the electronic effects of β -Cl or -Br substituents. 7,8,17,18-Cl₄ and 7,8,17,18-Br₄ substitutions of tetramesitylporphyrin elevate the oxidation potential by 0.24 and 0.21 V, respectively.¹⁷ These electrochemical SEs for β -tetrahalogenation are approximately half the LDF and XPS SEs for β -octahalogenation, which satisfactorily confirms the LDF results. Overall, Cl and Br substituents are seen to exert rather modest electronic effects on the porphyrin macrocycle. Thus, the enhanced stability of β -Cl₈ or β -Br₈ derivatives of metallotetraarylporphyrin complexes toward oxidants, relative to the unhalogenated metalloporphyrins, probably stems from a combination of the steric and electronic effects of the halogens.

β -Octafluorination has an effect of ca. 0.85 eV on the lowest IPs of PH₂, which exceeds the SEs due to β -Cl₈ or β -Br₈ substitution by a significant margin of 0.3–0.4 eV.⁵ The lowest LDF IP of perfluorinated TPPH₂ (F₂₈TPPH₂) exceeds that of ordinary TPPH₂ by as much as 1.65 eV!⁵ For comparison, the electrochemical oxidation potential of ZnF₂₈TPP exceeds that of ZnTPP by a significantly smaller but still large margin of 900 meV.¹⁸

Figure 6 also underscores the potential roles of cyano, nitro, and perfluoroalkyl substituents in designing super-electron-deficient porphyrins.⁵ For instance, *meso*-tetra-substitution with any of these substituents elevates the lowest IP of PH₂ by over 1 eV. The lowest IP of β -P(CN)₈H₂ exceeds that of PH₂ by 2 eV!

***meso*-Tetraarylporphyrins.** The LDF valence SEs for tetraarylporphyrins (obtainable from Figure 6) are in good agreement with HF and XPS SEs (Table 2). The LDF results confirm that substituents on the phenyl rings can

strongly modulate the electronic character of the porphyrin ring, although the phenyl rings are assumed to be perpendicular to the porphyrin plane. This suggests that the porphyrin–aryl electronic interaction has a significant dipolar component,¹⁹ although the nature of this interaction has not been probed in adequate detail. The data on the tetraarylporphyrins with fluorinated and nitro-substituted phenyl groups show that *ortho*, *meta*, and *para* substituents can exert significantly different SEs on porphyrin valence IPs. For the fluorinated tetraarylporphyrins, this probably stems from an angular dependence of dipolar electronic effects.¹⁹ In contrast, the surprisingly low first IP¹⁹ of *meso*-tetrakis(2,6-dinitrophenyl)porphyrin reflects stabilization of the ${}^2B_{1u}$ (A_{2u} -type) cationic state by direct orbital overlap interactions between the nitro oxygens and *meso* carbons.²⁰

Combined use of the LDF IP and existing electrochemical oxidation potential data on tetraarylporphyrins allows an evaluation of the importance of solvent effects. Kadish et al. obtained approximately linear Hammett plots of substituent-induced shifts in oxidation potentials (E) of free-base tetraarylporphyrins versus the sum of substituent constants ($\Sigma\sigma$) for the substituents on all four phenyl rings.²¹ The slopes, ρ , of such plots were 0.065 and 0.054 V for dichloromethane and *n*-butyronitrile solvents, respectively. In contrast, a Hammett plot of substituent-induced shifts in the lowest LDF IP of TPPH₂ versus $\Sigma\sigma$ has a slope of $\rho \approx 0.23$ eV, which is considerably higher than the slopes found for the electrochemical plots.⁵ Thus, *p*-fluoro and *p*-cyano substitution of all four phenyl rings of TPPH₂ increases the electrochemical oxidation potential by ~ 0.1 and 0.2 V, respectively, but affects the LDF first IP by 0.29 and 0.76 eV, respectively. What causes this discrepancy between electrochemical and LDF substituent effects? While a definitive answer must await UPS measurements, two facts argue against the possibility that LDF theory is inadequate. First, LDF theory has performed astonishingly well in reproducing the lowest one-electron IPs of porphyrins for which experimental UPS data are available.^{5,15} Second, the electronic effects of phenyl substituents on the lowest LDF IPs of TPPH₂ are about equal to substituent effects on experimental XPS N 1s core IPs.^{5,7} This suggests that substituent effects on electrochemical oxidation potentials can differ significantly from shifts in gas-phase IPs, especially where these shifts are very large. Overall, solvation appears to exert a moderating effect on substituent effects in porphyrins.⁵

Structural Studies of Porphyrinoids

Structural studies of porphyrin-type molecules with first-principles quantum chemical methods are a relatively recent development. Until recently, there was considerable confusion as to the choice of a suitable quantum chemical method for such studies. Thus, both semiempirical theories²² such as QCFF/PI, spin-restricted AM1, and PM3 and ab initio Hartree–Fock theory²³ result in unrealistic symmetry-broken structures of porphyrinoids with alternating localized single and double bonds. Sym-

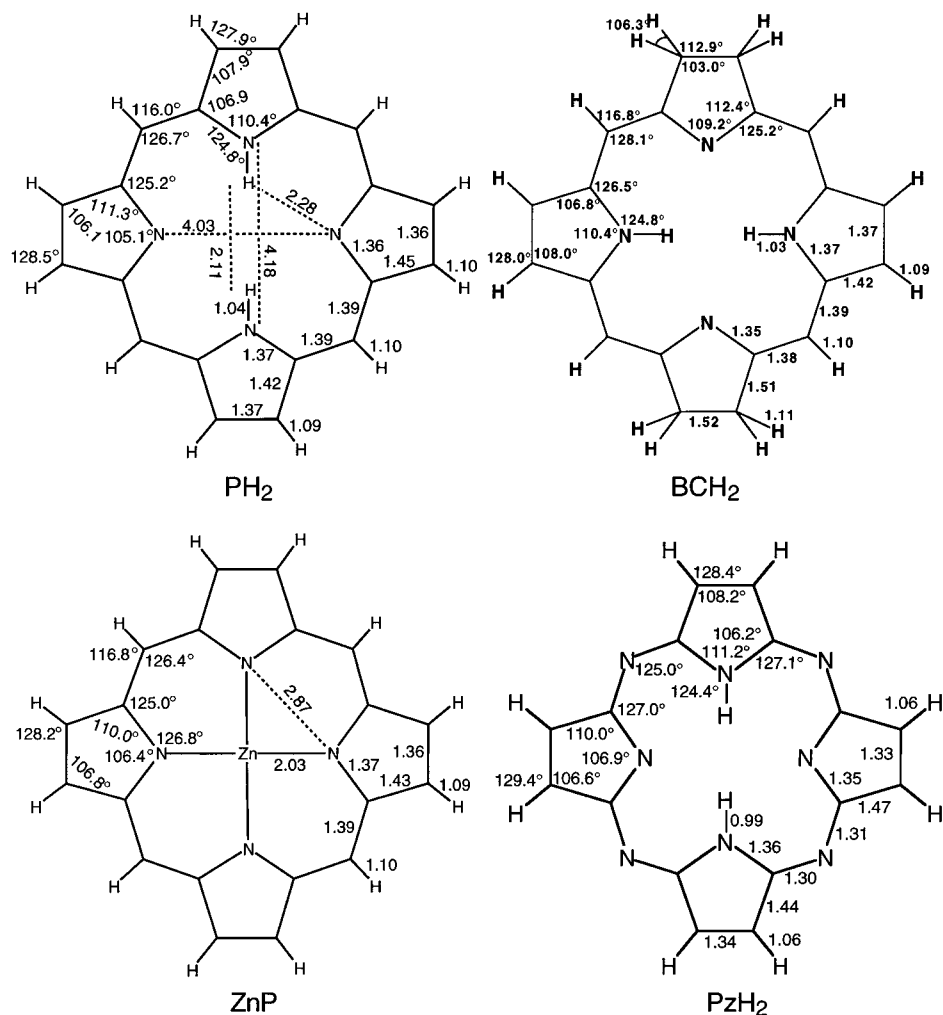


FIGURE 7. Optimized geometries (Å, deg) of some common porphyrinoids.

metry-constrained realistic structures of porphyrins have one or more imaginary frequencies at these levels of theory. In 1993, we reported that simple schemes of electron correlation such as second-order Møller–Plesset perturbation theory (MP2) and DFT can rectify this problem and yield realistic delocalized optimized geometries.^{23a} Other workers have subsequently confirmed this finding using DFT vibrational analyses²⁴ and multiconfigurational perturbation theory (CASPT2) calculations.²⁵ Since this discovery, quantum chemistry, especially DFT, has emerged as an important tool for structural studies of porphyrin-type molecules.

Figure 7 depicts LDF/DZP optimized geometries of some common porphyrinoids. The order of bond lengths in PH_2 ²³ and ZnP ²⁶ is $C_\alpha\text{--}C_\beta$ (1.42–1.45 Å) > $C_\alpha\text{--}C_{\text{meso}}$ (1.39 Å) > $C_\beta\text{--}C_\beta \approx C_\alpha\text{--}N$ (1.36–1.37 Å). Note the long $C_\alpha\text{--}C_\beta$ bonds, a well-known peculiarity of porphyrins. Both the $C_\alpha\text{--}C_\beta$ and $C_\beta\text{--}C_\beta$ bonds (1.51–1.52 Å) in the reduced rings of hydroporphyrins such as BCH_2 have lengths typical of single bonds. The $\alpha\text{--meso}$ distances in PzH_2 ¹⁰ are short (1.30–1.31 Å) relative to those in PH_2 . Thus, PzH_2 has a smaller N_4 core and a stronger ligand field, which may explain the unusual $S = 3/2$ spin state for $\text{OEPzFe}^{\text{III}}\text{Cl}$ (cf. five-coordinate Fe^{III} porphyrins, which are high-spin).²⁷ The $C_\alpha\text{--}N\text{--}C_\alpha$ angles are significantly

larger in the N-protonated pyrrole rings of PH_2 than in the N-unprotonated rings, 110.4° versus 105.1° .²³ In contrast, the $C_\alpha\text{--}N\text{--}C_\alpha$ angles are fairly uniform ($109.2\text{--}110.4^\circ$) across all four rings in BCH_2 .¹³ Thus, hydrogenation of a $C_\beta\text{--}C_\beta$ bond results in a widening of the $C_\alpha\text{--}N\text{--}C_\alpha$ angle and, therefore, also a slight increase in distance of the nitrogen of the reduced ring from the macrocycle center. Increased metal–nitrogen bond distances involving the reduced rings of bacteriochlorins, relative to analogous distances for porphyrins, have been noted in crystallographic studies.²⁸ Overall, theory and crystallography are in excellent agreement with regard to many detailed structural features of the common porphyrinoids. This encouraged us to undertake DFT geometry optimization studies of other more interesting and exotic porphyrinoids.

NH Tautomerism. Figure 8 depicts various species relevant to NH tautomerism in PH_2 and monodeprotonated porphine, PH^- . The double proton migration in PH_2 is believed to be a stepwise process,²⁹ and an energy of ca. 8 kcal/mol has been calculated for the *cis*- PH_2 intermediate at LDF, nonlocal DFT, and MP2 levels.^{30,31} The transition state between *cis* and ordinary PH_2 has been calculated to lie ca. 17 kcal/mol above PH_2 at the nonlocal DFT level.³¹ Consistent with the experimental observation

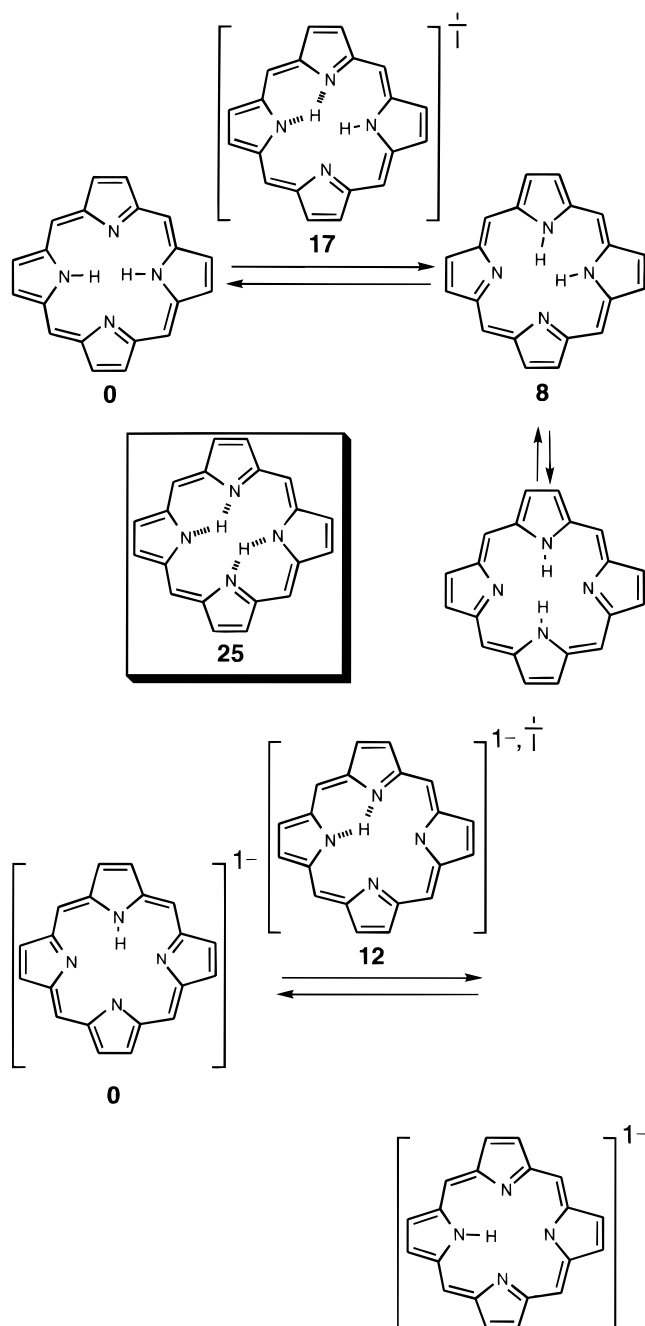


FIGURE 8. Some stationary points on the potential energy surfaces of PH_2 and PH^- , along with their NLDFT relative energies (kcal/mol).

that the tautomerism is significantly faster in PH^- than in PH_2 ,³² the proton-transfer transition state of PH^- has been found to be 11 kcal/mol above the ground state at the nonlocal DFT level.³³ The ground states of PH_2 and PH^- feature symmetrical bifurcated hydrogen bonding, the N–H bond lengths and $\text{NH}\cdots\text{N}$ contacts being 0.99 and ca. 2.3 Å, respectively, for either molecule.^{23,33} In the transition states, the $\text{N}\cdots\text{H}$ contacts involving the migrating hydrogen are ca. 1.33 Å.^{31,33} The skeletal geometries of PH_2 and PH^- distort significantly in the course of the proton transfer, with the bond angles of the central C_{12}N_4 ring undergoing the maximum changes.^{30,31,33}

Porphyrin Isomers. Theory has shed considerable light on thermochemical and structural aspects of por-

phyrin isomers.³⁴ BLYP/6-31G**//3-21G calculations³⁵ predict rather low energies for the [2.0.2.0],^{36a} [2.1.1.0],^{36b} [2.1.0.1],^{36c} and *cis*- and *trans*-[3.0.1.0]^{36d} isomers relative to PH_2 , consistent with the successful syntheses³⁶ of each of these ring systems (Figure 9). Using LDF/DZP optimizations, we have studied the possibility of skeletal *cis*–*trans* isomerism in porphyrin isomers.³⁷ Very recently, this possibility has been experimentally realized with the observation of a rapid photochemical equilibrium between the *cis*- and *trans*-[3.0.1.0]porphyrin stereoisomers.^{36d} Yet to be experimentally observed is *trans*-[3.1.0.0]porphyrin with an energy of 26.6 kcal/mol relative to PH_2 at the LDF level. In contrast, *cis*-[3.1.0.0]porphyrin has a significantly higher energy, 39.3 kcal/mol relative to PH_2 at the LDF level, and it is doubtful if this stereoisomer can at all be synthesized. Similarly, the energies of both *cis* and *trans* stereoisomers of [4.0.0.0]porphyrin appear to be too high to permit their isolation. Examples of significant sources of strain in the structures of porphyrin isomers are certain large bond angles subtended at the (CH_3) interpyrrole linker in the [3.0.1.0] and [3.1.0.0] isomers and rather long direct C_α – C_α and other CC bonds in the interpyrrole bridges (1.39–1.43 Å) (compare C_α – C_{meso} in PH_2 , which is 1.38 Å) (Figure 9).³⁷

Corrole Isomers. LDF geometry optimizations have also been used to study corrole isomers (Figure 10).²⁶ Table 3 presents calculated thermochemical data on the free bases and Ga^{III} , In^{III} , and Sc^{III} complexes of corrole isomers, and Figure 10 also includes selected optimized geometries. Normal corrole, or [1.1.1]corrole,³⁸ which has bond lengths generally similar to those in PH_2 , is the most stable isomer for both free-base and metal-complexed series. The stretched C_α – C_α linkages and wide exocyclic $\text{C}_\beta\text{C}_\alpha\text{C}_\alpha$ angles at these linkages are a principal source of strain in the normal and isomeric corrole structures, as in certain porphyrin isomers.³⁷ Moderately low energies are also predicted for the [2.0.1] and [2.1.0] isomers, consistent with the actual synthesis of the [2.0.1]corrole or isocorrole ring system.³⁹ The higher energies of these isomers relative to [1.1.1]corrole are related to the presence of two direct C_α – C_α linkages in the former compounds. The size of the N_4 core also plays a crucial part in determining the relative energetics of metalcorrole isomers.²⁶ Normal corroles and [2.0.1]corroles have a small N_4 core. The short optimized Ga–N distances of ca. 1.9 Å in [1.1.1]CorGa and [2.0.1]CorGa are typical of metal–nitrogen distances in metalcorroles but shorter than those typically found in metalloporphyrins. In contrast, the [2.1.0] isomer, with an unsymmetrical core and a relatively long separation between two diagonally opposite nitrogens, is expected to coordinate optimally with a larger metal ion such as Sc^{III} or In^{III} . These structural features explain the reversal of the relative stabilities of [2.0.1]- and [2.1.0]metalcorroles with increasing metal ion size.²⁶ The *cis* and *trans* stereoisomers of [3.0.0]corrole have high molecular energies, and their actual isolation seems doubtful. Except for *trans*-[3.0.0]-corrole derivatives, all the corrole isomers and their metal complexes have relatively planar geometries. Finally, for

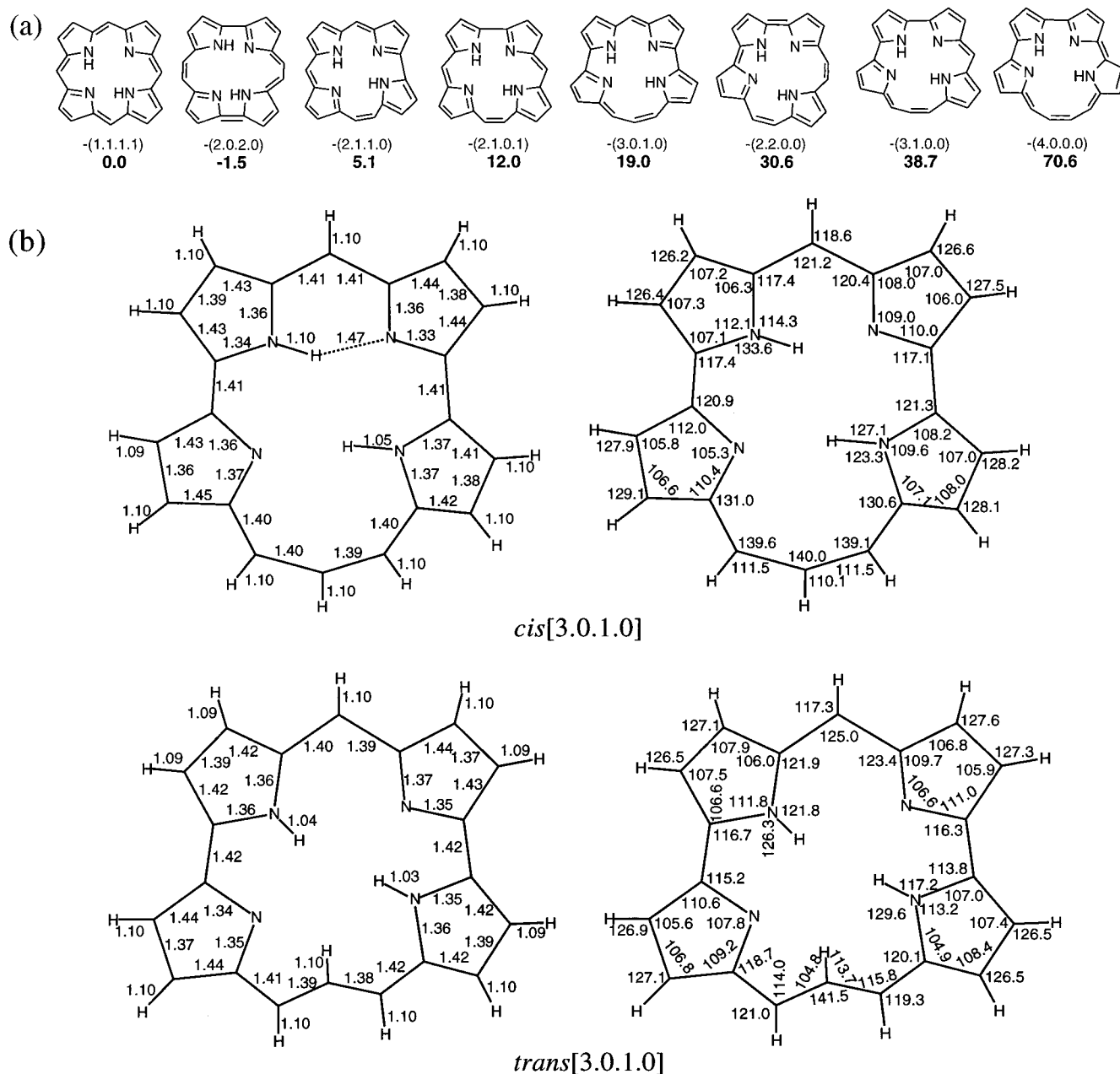


FIGURE 9. (a) Molecular structures and calculated relative energies (kcal/mol, BLYP/6-31G**//3-21G, shown in bold) of the stable tautomers of selected porphyrin isomers. Reprinted with permission from ref 37. Copyright 1997 American Chemical Society. (b) Selected optimized geometries (Å, deg).

any particular corrole isomer, the NH tautomers are of similar energy, differing by 2–7 kcal/mol.²⁶ For instance, the two tautomers of normal corrole differ by only 2.45 kcal/mol at the LDF/DZP level, and both feature short, strong NH···N hydrogen bonds. Thus, one may expect very fast NH tautomerism in normal corrole, and similar considerations apply also to the other corrole isomers.

Carbaporphyrins. Geometry optimizations and other DFT calculations⁴⁰ have played an important role in clarifying the remarkable chemical properties of carbaporphyrins.^{41,42} Interest in the 2-aza-21-carbaporphyrins (**A**, Figure 11), also called inverted or N-confused porphyrins, centers on their ability to act as tetracoordinate ligands and form complexes (e.g., **B**, Figure 11) with metal–carbon bonds.⁴⁴ What accounts for the surprising

carbon acidity of an inverted porphyrin? LDF calculations including geometry optimization indicated that the C-deprotonated tautomer **C** (Figure 11) has the electronic characteristics of a typical heteroatom-stabilized nucleophilic singlet carbene.⁴³ The $\sigma^1\pi^1$ triplet, derived by excitation of **C**'s carbenic lone pair, is higher than the ground singlet by ca. 41 kcal/mol, which is close to the singlet–triplet splitting for CF_2 , a typical singlet carbene.⁴³ Similarly, the IP of the carbenic lone pair of **C** is calculated to be 7.31 eV, close to that found experimentally for the “bottleable” *N,N*-dialkylimidazol-2-ylidenes.⁴⁴ These indicators of the electronic stability of the carbenic lone pair of **C** provide a partial explanation of the ease of formation of **B**, which may be regarded as a complex of **C**. It needs to be emphasized, however, that we do not suggest that **C** is

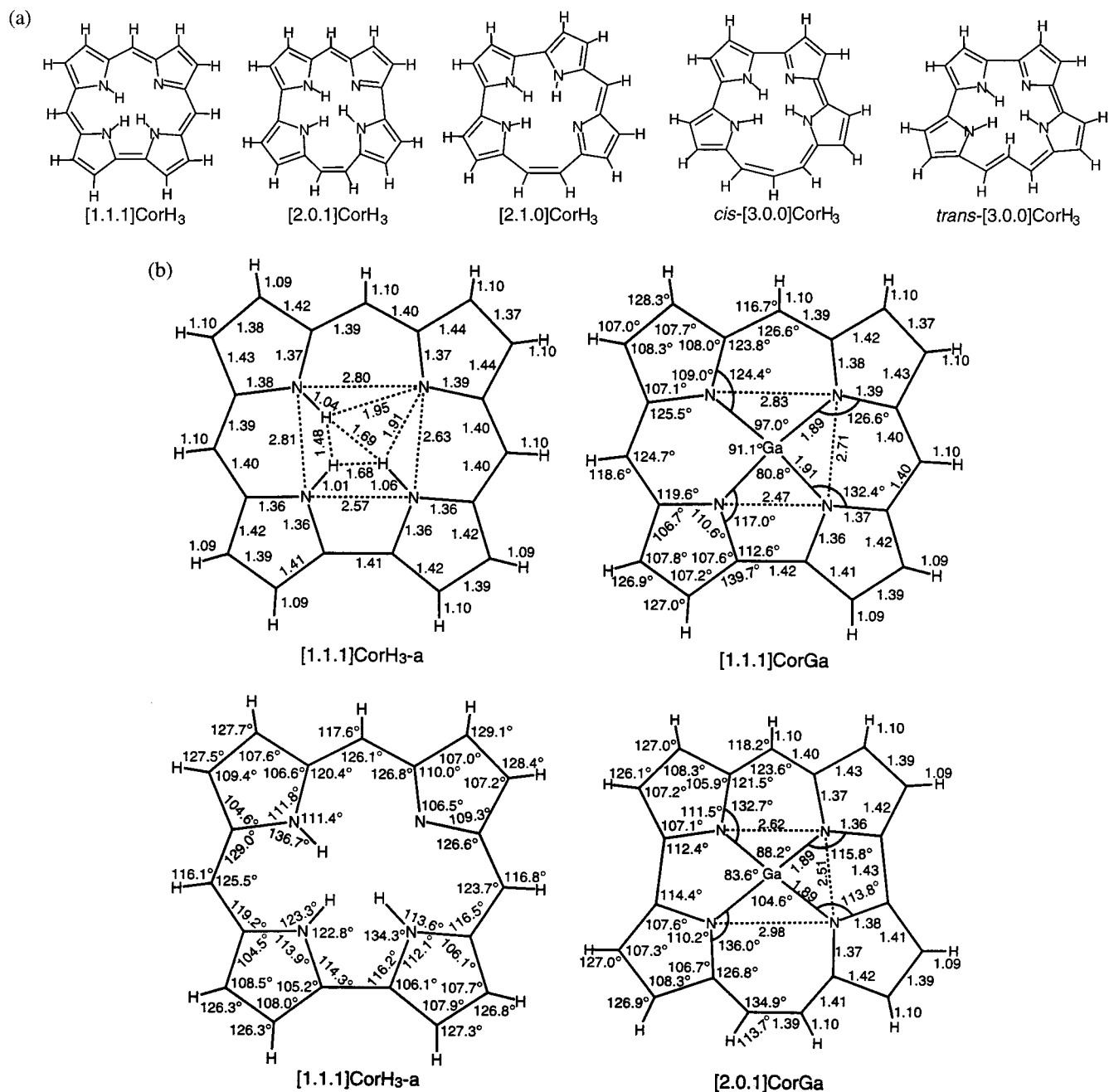


FIGURE 10. (a) Stable tautomers of some corrole isomers. (b) Selected optimized geometries (Å, deg).

Table 3. LDF/DZP Energies (kcal/mol) of Free-Base and Ga^{III}, In^{III}, and Sc^{III} Complexes of Corrole Isomers Relative to the Normal Corrole Derivatives^a

isomer	free-base	Ga ^{III}	Sc ^{III}	In ^{III}
[1.1.1]	0.0	0.0	0.0	0.0
[2.0.1]	7.9	13.5	11.1	23.1
[2.1.0]	18.1	27.0	13.1	15.8
<i>cis</i> -[3.0.0]	50.7	63.2	33.6	56.4
<i>trans</i> -[3.0.0]	43.9	70.0	15.7	47.3

^a For details of geometry optimizations, see ref 27.

an intermediate in the reaction path leading to **B**. The formation of **B** must also involve Ni^{II}-assisted CH activation, since a highly favorable orbital overlap can be expected between the carbenic lone pair of **C** and the empty $d_{x^2-y^2}$ orbital of square planar Ni^{II}.⁴⁰

Omissions

In this Account, the emphasis has been on describing the ground states of mostly metal-free tetrapyrroles. We have largely ignored transition metal porphyrins and porphyrin excited states, two important aspects of porphyrin chemistry. Ab initio studies of both of these areas require the use of high-quality correlated methods, a difficult task in view of the size of porphyrin-type molecules. Currently, DFT is probably the most convenient tool for studies of ground-state potential energy surfaces of transition metal porphyrins. Recent DFT studies in this area from our laboratory include studies of ferryl intermediates⁴⁵ and the question of deformability of the Fe^{II}CO and Fe^{III}CN groups

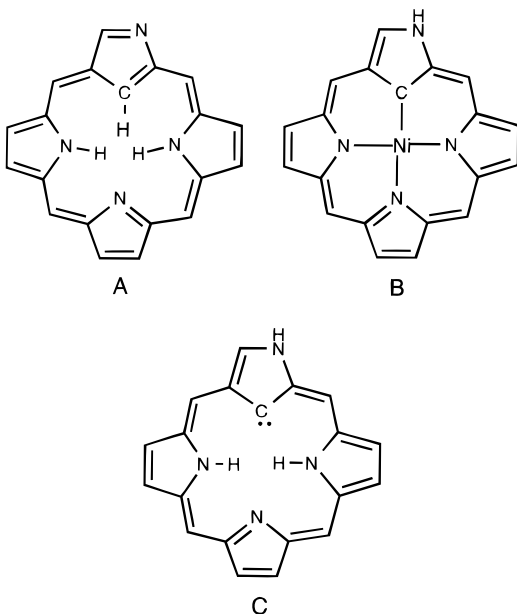


FIGURE 11. Carbaporphyrin structures.

in heme protein models.⁴⁶ Other research groups have studied the electronic spectra of porphyrins with multi-configurational perturbation theory,⁴⁷ configuration interaction,⁴⁸ coupled cluster,⁴⁹ and time-dependent DFT⁵⁰ methods. However, a number of these calculations have been performed with relatively small basis sets, and discrepancies between calculated and experimental electronic absorption features have been as large as 0.5 eV. These excited-state calculations constitute a significant advance in theoretical porphyrin research. Finally, preliminary studies in our laboratory indicate that DFT reproduces well the gas-phase electron affinities of a variety of porphyrins.²⁰

Concluding Remarks

DFT and, to some extent, *ab initio* HF calculations have provided new insights into diverse aspects of porphyrin chemistry such as ionization and oxidation potentials, photoelectron spectra, substituent effects, and the molecular structures and thermochemistry of porphyrin isomers and analogues. Electron correlation plays a crucial role in determining most calculated properties of porphyrin-type molecules, and DFT has served as an affordable and excellent correlated method in this regard. Traditional *ab initio* correlated calculations, currently somewhat impractical, remain an important goal for the future.

This research is supported by the Norwegian Research Council, the VISTA program of Statoil-Norway, and a Senior Fellowship of the San Diego Supercomputer Center. It is a pleasure to record my gratitude to my collaborators whose names are cited in the appropriate references.

References

- (1) Mashiko, T.; Dolphin, D. Porphyrins, Hydroporphyrins, Azaporphyrins, Phthalocyanines, Corroles, Corrins, and Related Macrocycles. In *Comprehensive*

- Coordination Chemistry*; Wilkinson, G., Chief Editor; Pergamon: Oxford, 1987; Vol. 2, Chapter 21.1, p 813.
- (2) Hanson, L. K. *Photochem. Photobiol.* **1988**, *47*, 903.
- (3) Dolphin, D.; Traylor, T. G.; Xie, L. Y. *Acc. Chem. Res.* **1997**, *30*, 251.
- (4) *Metalloporphyrins in Catalytic Oxidations*; Sheldon, R. A., Ed.; Marcel Dekker: New York, 1994.
- (5) Ghosh, A. *J. Am. Chem. Soc.* **1995**, *117*, 4691.
- (6) Ghosh, A.; Almlöf, J.; Gassman, P. G. *Chem. Phys. Lett.* **1991**, *186*, 113.
- (7) Gassman, P. G.; Ghosh, A.; Almlöf, J. *J. Am. Chem. Soc.* **1992**, *114*, 9990.
- (8) (a) Dupuis, P.; Roberge, R.; Sandorfy, C. *Chem. Phys. Lett.* **1980**, *75*, 434. (b) Kitagawa, S.; Morishima, I.; Yonezawa, T.; Sato, N. *Inorg. Chem.* **1979**, *18*, 1345.
- (9) Gouterman, M. In *The Porphyrins*; Dolphin, D., Ed.; Academic: New York, 1978; Vol. III, Part A, Physical Chemistry.
- (10) Ghosh, A.; Gassman, P. G.; Almlöf, J. *J. Am. Chem. Soc.* **1994**, *116*, 1932.
- (11) Ghosh, A.; Fitzgerald, J.; Gassman, P. G.; Almlöf, J. *Inorg. Chem.* **1994**, *33*, 6057–6060.
- (12) Ghosh, A. *J. Phys. Chem.* **1994**, *98*, 11004.
- (13) Ghosh, A. *J. Phys. Chem. B* **1997**, *101*, 3290.
- (14) (a) Gunnarsson, O.; Lundqvist, B. I. *Phys. Rev. B* **1976**, *13*, 4274. (b) Ziegler, T.; Rauk, A.; Baerends, E. J. *Theor. Chem. Acta* **1977**, *43*, 261. (c) Jones, R. O.; Gunnarsson, O. *Rev. Mod. Phys.* **1989**, *61*, 689.
- (15) Ghosh, A.; Almlöf, J. *Chem. Phys. Lett.* **1993**, *213*, 519.
- (16) Ghosh, A.; Vangberg, T. *Theor. Chem. Acc.* **1997**, *97*, 143.
- (17) Ochsenein, P.; Ayougou, K.; Mandon, D.; Fischer, J.; Weiss, R.; Austin, R. N.; Jayaraj, K.; Gold, A.; Turner, J.; Fajer, J. *Angew. Chem., Int. Ed. Engl.* **1994**, *33*, 348.
- (18) Woller, E. K.; DiMugno, S. G. *J. Org. Chem.* **1997**, *62*, 1588.
- (19) Ghosh, A. *J. Mol. Struct.: THEOCHEM* **1996**, *288*, 359.
- (20) Vangberg, T.; Ghosh, A. Unpublished results.
- (21) Kadish, K. M. In *Progress in Inorganic Chemistry*; Lippard, S. J., Ed.; Wiley: New York, 1986; p 435.
- (22) (a) Zerbetto, F.; Zgierski, M. Z.; Orlandi, G. *Chem. Phys. Lett.* **1987**, *139*, 401. (b) Reynolds, C. H. *J. Org. Chem.* **1988**, *53*, 6061.
- (23) (a) Almlöf, J.; Fischer, T. H.; Gassman, P. G.; Ghosh, A.; Häser, M. *J. Phys. Chem.* **1993**, *97*, 10964. (b) Piqueras, M. C.; Rohlffing, C. M. *J. Mol. Struct.* **1996**, *388*, 293. (c) Piqueras, M. C.; Rohlffing, C. M. *Theor. Chem. Acc.* **1997**, *97*, 81.
- (24) (a) Kozłowski, P. M.; Zgierski, M. Z.; Pulay, P. *Chem. Phys. Lett.* **1995**, *247*, 379. (b) Kozłowski, P. M.; Jarzecki, A. A.; Pulay, P. *J. Phys. Chem.* **1996**, *100*, 7007. (c) Kozłowski, P. M.; Jarzecki, A. A.; Pulay, P.; Li, X.-Y.; Zgierski, M. Z. *J. Phys. Chem.* **1996**, *100*, 13985.
- (25) Merchan, M.; Orti, E.; Roos, B. O. *Chem. Phys. Lett.* **1994**, *221*, 136.
- (26) Ghosh, A.; Jynge, K. *Chem. Eur. J.* **1997**, *3*, 823.
- (27) Ghosh, A.; Fitzgerald, J.; Gassman, P. G.; Almlöf, J. *Inorg. Chem.* **1994**, *33*, 6057.
- (28) Barkigia, K. M.; Fajer, J. In *The Photosynthetic Reaction Center*; Deisenhofer, J., Norris, J. R., Eds.; Academic Press: San Diego, CA, 1993; Vol. 2, p 513.
- (29) *Theoretical work*: (a) Kuzmitsky, V. A.; Solov'yov, K. N. *J. Mol. Struct.* **1980**, *65*, 219. (b) Sarai, A. *J. Chem. Phys.* **1982**, *76*, 5554. (c) Merz, K. M.; Reynolds, C. H. *J. Chem. Soc., Chem. Commun.* **1988**, 90. (d) Smedarchina, Z.; Siebrand, W.; Zerbetto, F. *Chem.*

- Phys.* **1989**, *136*, 285. Experimental work: (e) Butenhoff, T.; Moore, C. B. *J. Am. Chem. Soc.* **1988**, *110*, 8336. (f) Butenhoff, T.; Chuck, R.; Limbach, H.-H.; Moore, C. B. *J. Phys. Chem.* **1990**, *94*, 7487.
- (30) Ghosh, A.; Almlöf, J. *J. Phys. Chem.* **1995**, *99*, 1073.
- (31) Baker, J.; Kozłowski, P. M.; Pulay, P. *Theor. Chem. Acc.* **1997**, *97*, 59.
- (32) Braun, J.; Hasenfratz, C.; Schwesinger, R.; Limbach, H. H. *Angew. Chem., Int. Ed. Engl.* **1994**, *33*, 2215.
- (33) Vangberg, T.; Ghosh, A. *J. Phys. Chem. B* **1997**, *101*, 1496.
- (34) Vogel, E. *J. Heterocycl. Chem.* **1996**, *33*, 1461.
- (35) Vogel, E.; Bröring, M.; Fink, J.; Rosen, D.; Schmickler, H.; Lex, J.; Chan, K. W. K.; Wu, Y.-D.; Plattner, D. A.; Nendel, M.; Houk, K. N. *Angew. Chem., Int. Ed. Engl.* **1995**, *34*, 2511.
- (36) (a) Vogel, E.; Köcher, M.; Schmickler, H.; Lex, J. *Angew. Chem., Int. Ed. Engl.* **1986**, *25*, 257. (b) Sessler, J. L.; Brucker, E. A.; Weghorn, S. J.; Kisters, M.; Schäfer, M.; Lex, J.; Vogel, E. *Angew. Chem., Int. Ed. Engl.* **1994**, *33*, 2308. (c) Callot, H. J.; Rohrer, A.; Tschamber, T.; Metz, B. *New J. Chem.* **1995**, *19*, 155. (d) Vogel, E.; Bröring, M.; Erben, C.; Demuth, R.; et al. *Angew. Chem., Int. Ed. Engl.* **1997**, *36*, 353.
- (37) (a) Ghosh, A.; Jynge, K. *J. Phys. Chem. B* **1997**, *101*, 5459. (b) A more extensive theoretical study of porphyrin isomers has appeared since the initial submission of this Account: Wu, Y.-D.; Chan, K. W. K.; Yip, C.-P.; Vogel, E.; Plattner, D. A.; Houk, K. N. *J. Org. Chem.* **1997**, *62*, 9240.
- (38) Licoccia, S.; Paolesse, R. *Struct. Bond.* **1995**, *84*, 71.
- (39) Will, S.; Rahbar, A.; Schmickler, H.; Lex, J.; Vogel, E. *Angew. Chem., Int. Ed. Engl.* **1990**, *29*, 1390.
- (40) (a) Ghosh, A. *Angew. Chem., Int. Ed. Engl.* **1995**, *34*, 1028. (b) Nilsen, H. J.; Ghosh, A. *Acta Chem. Scand.*, in press.
- (41) Chmielewski, P. J.; Latos-Grazynski, L.; Rachlewicz, K.; Glowiak, T. *Angew. Chem., Int. Ed. Engl.* **1994**, *33*, 779.
- (42) Furuta, H.; Asano, T.; Ogawa, T. *J. Am. Chem. Soc.* **1994**, *116*, 767.
- (43) King, H. F.; Komornicki, A. *J. Chem. Phys.* **1986**, *84*, 5465.
- (44) Arduengo, A. J.; Bock, H.; Chen, H.; Denk, M.; Dixon, D. A.; Green, J. C.; Herrman, W. A.; Jones, N. L.; Wagner, M.; West, R. *J. Am. Chem. Soc.* **1994**, *116*, 6641.
- (45) Ghosh, A.; Almlöf, J.; Que, L., Jr. *J. Phys. Chem.* **1994**, *98*, 5576.
- (46) (a) Ghosh, A.; Bocian, D. F. *J. Phys. Chem.* **1996**, *100*, 6363–6367. (b) Vangberg, T.; Bocian, D. F.; Ghosh, A. *J. Biol. Inorg. Chem.* **1997**, *2*, 526.
- (47) Merchan, M.; Orti, E.; Roos, B. O. *Chem. Phys. Lett.* **1994**, *226*, 27.
- (48) (a) Nakatsuji, H.; Hasegawa, J. Y.; Hada, M. *J. Chem. Phys.* **1996**, *104*, 2321. (b) Hasegawa, J. Y.; Hada, M.; Nonoguchi, M.; Nakatsuji, H. *Chem. Phys. Lett.* **1996**, *250*, 159. (c) Nakatsuji, H.; Hasegawa, J. Y.; Ueda, H.; Hada, M. *Chem. Phys. Lett.* **1996**, *250*, 437. (d) Toyota, K.; Hasegawa, J.; Nakatsuji, H. *Chem. Phys. Lett.* **1996**, *250*, 437. (e) Nakatsuji, H.; Tokita, Y.; Hasegawa, J. Y.; Hada, M. *Chem. Phys. Lett.* **1996**, *256*, 220. (f) Toyota, K.; Hasegawa, J.; Nakatsuji, H. *J. Phys. Chem. A* **1997**, *101*, 446. (g) Tokita, Y.; Nakatsuji, H. *J. Phys. Chem. B* **1997**, *101*, 3281.
- (49) Nooijen, M.; Bartlett, R. J. *J. Chem. Phys.* **1997**, *106*, 6449.
- (50) Bauernschmitt, R.; Ahlrichs, R. *Chem. Phys. Lett.* **1996**, *256*, 454.

AR950033X